ActaEnergetica
POWER ENGINEERING QUARTERLY

Model Designing of Analog Integrated Circuits for the Physiological Signals

Jakub Siemek
DSc(Eng), Professor, The AGH University of Science and Technology, Kraków, Poland

Dr. Prakash Pise
Sinhgad Institute of Management,
SPPU PUNE UNIVERSITY, India
prakash.pise532@gmail.com

Keywords
Analog integrated Circuits, Bulk-driven MOSFETs, Low Power methods, Physiological Signals

Abstract
For processing physiological data, analogue integrated circuits (ICs) are essential components of wearable and implantable medical devices used for health monitoring or restoring lost body functions. Physiological signal characteristics and related application scenarios require low input-referred noise, low power consumption, and low cutoff frequency in ICs designed for these applications. This work describes how to build fully integrated circuits for low cutoff frequencies, chopper stabilization (CHS), and other techniques that can be used to generate high signal-to-noise ratios. To reduce power consumption, these techniques include subthreshold circuits, bulk-controlled MOSFETs, floating-gate MOSFETs, and log-domain circuits. New applications of these methods are also described.

Received by the editor: 18.07.2022
Received in revised form: 04.10.2022
Accepted: 25.10.2022

1. INTRODUCTION

The ageing of the global population and the development of chronic diseases have significantly strained our current healthcare systems. Meanwhile, there is a pressing need for a more proactive healthcare strategy in which a person's health is closely monitored from birth in order to avoid, anticipate, identify, and cure disorders as soon as possible. Wearable and implantable devices, which must be small and discreet enough to allow users to continue living their usual lives without interruption, provide long-term and continuous monitoring of health issues. Six enabling technologies are needed to make these gadgets possible: downsizing, integration, networking, digitalization, smarts, and standardisation (MINDSS).

For these wearable and implantable devices to carry out a variety of tasks, including processing physiological signals, integrated circuits (ICs) were designed and implemented. This is referred to as integration in the description above.

Biological signals, for example, biopotentials like electrocardiograms (ECG), electroencephalograms (EEG), and electromyograms (EMG), as well as synthetic and actual amounts like particle concentrations and body temperatures and blood pressure, are frequently brief and low-frequency signals. Hence, a simple front-end circuit is every now and again expected to channel and intensify the sign prior to digitizing it for additional processing. This is finished in the wake of changing a physiological contribution to an electrical sign by means of the suitable kind of sensor or transducer.

A. Low Power Design Method

By lowering the stockpile voltage, diminishing the activity current, or compacting the sign from the ongoing area to the voltage space using the remarkable semiconductor current versus voltage connection, decreased power utilization can be accomplished.

- Low Threshold Voltage Methods

One more technique to scale back energy use is to lower the stock voltage. In any case, since this would build the off-state or static spillage of advanced circuits, edge voltage can't be downsized at a similar rate as supply voltage with expanding highlight size. In the event that the edge voltages can't be downsized with supply voltages at similar speed, the confined voltage headroom at low stock voltages would introduce huge issues to simple IC designers. Low identical limit voltages, which compare to low inventory voltages, have been accomplished by the utilization of certain methodologies.

1) Bulk-driven MOSFETs:To provide low transconductance and improve circuit linearity, Guzinski et al. [34]. Their ideas have recently evolved into techniques for lowering edge voltages in low-power circuit designs.

In a customary MOSFET, the impact of mass to source voltage is exclusively considered as a parasitic impact and channel current is constrained by gate to source voltage. As opposed to the regular arrangement, as portrayed in Fig. 3(a), a mass driven MOSFET is constrained by a consistent. The inclination voltages for a mass driven MOSFET, which proceeds as a JFET-like semiconductor, can be negative, zero, or just marginally sure. The following [38] ought to be considered while designing low power circuits using mass driven MOSFETs: Just PMOSFET and NMOSFET are accessible in N-well processes and P-well processes, separately, on the grounds that mass driven MOSFETs are process-subordinate; 2) ought to be lower than the turn-on voltage of the mass channel PN intersection; in any case, parasitic bipolar intersection semiconductor (BJT) lock up may happen while is expanding; 3. Mass driven MOSFETs perform more awful as far as recurrence attributes and transconductance when contrasted with gate-driven semiconductors. 4. Mass driven MOSFETs perform more terrible as far as equivalent information induced commotion when contrasted with gate-driven MOSFETs.

Bulk -drive MOSFETs are useful for building low-voltage, low-power circuits for biomedical applications. With NMOSFET and PMOSFET cutoff voltages of 0.5 V and 0.65 V, respectively, Lasanen et al. [39] used a mass-driven P-type input-differential pair in a 0.35 µm N-well CMOS process for biomedical applications. Built a functional 1 V, 0.5 W loudspeaker for equipment. The intensifier's feedback well known mode range was expanded, and the edge voltage was extraordinarily diminished. The viewpoint proportion of the mass driven MOSFET was made to be pretty much as extensive as conceivable to forestall the source to mass and source to substrate spillage flows as well as the parasitic BJT hook up. An exceptional OTA with twin mass driven input stages in a 0.35-m CMOS innovation with a 0.9 V stock and 9.9 W power utilization was likewise proposed by Container et al. [40]. The imaginative method forestalled the spillage current of conventional mass driven circuits while accomplishing a rail-to-rail input range. A promising construction for low power and low voltage biomedical applications is the mass driven MOSFET.

2) Floating Gate MOSFETs: Since Kahng and Sze's 1967 [41] proposition of the drifting gate MOS (FGMOS) structure as a nonvolatile memory gadget, it has been broadly used in computerized EPROM and EEPROM. The controlling gate is capacitively associated with the drifting gate, which is encircled by SiO with no electrical associations. The controlling gate gets the info signal. By appropriately changing the info voltage, the powerful edge voltage can be diminished to a modest number. Thus, a tunable and lower limit voltage has as of late been found in the low voltage and low power domain.

B. Low Frequency Design Methods

Low frequency transmissions are the majority of physiological signals. Because of this, it is frequently necessary to design circuits with high time constants (r = RC or T = C/gm), which requires the implementation of large capacitances, enormous protections, and/or little transconductances (most commonly alluding to the transconductances of OTAs). As per the condition 1A2x-RC, the base region expected to accomplish an end recurrence of 1 Hz utilizing the UMC 0.13-pm CMOS process,

where a 1-pF capacitor and a bla resistor involve 10 — 3 mm2 and 10-6 mm2, individually, is 0.8 mm2. This is valid in any event, when a 400-pF capacitor and a 0.4-al resistor are utilized. The resistor and capacitor have a sizable consolidated surface region. On the other hand, a 100 pF capacitor and a 0.628 rus/V transconductance in light of &ANC) can likewise be utilized to make an end recurrence of 1 Hz, assuming that 100 pF is the most extreme allowable incentive for the capacitor. Be that as it may, building OTAs with transconductances below 1 nA/V is comparably troublesome, especially when chip space, clamor execution, and dynamic reach are undeniably considered. To handle the previously mentioned issues, certain exceptional arrangements have been investigated.

- MOS Pseudo-Resistor

A MOSFET one-sided in the subthreshold district can deliver an obstruction of many uber ohms. In brain recording circuits, this kind of MOS resistor is habitually utilized related to a capacitor to brace huge dc float at the recording site. Utilizing a NMOSFET driven in the subthreshold locale and a terminal capacitance, Chandran et albrain .'s recording enhancer [54] had the option to get an end recurrence below 20 Hz. The exhibition of the speaker is unaffected by a dc input voltage in the scope of 0 to 0.4 V. Negative dc inputs, nonetheless, can't be dismissed by the design. With the assistance of a recording test capacitance of around 22 pF and a PMOSFET driven in the subthreshold district, Mohseni et al. [55] introduced a superior brain recording intensifier utilizing the dc standard adjustment method, lowering the end recurrence below 50 Hz. It was resolved that the adequate scope of dc inputs was something like 0.25 V. Resistors were utilized in these two designs [54], [55] to predisposition the MOS resistors. The end frequencies of these biasing resistors were made movable by laser managing. With no biasing circuit and diode connected subthreshold NMOSFETs with an identical opposition more prominent than 15.9, Olsson et al[56] .'s brain recording intensifier was made. The allowable scope of dc input voltages was estimated to be 0.5 V, and the lower-band cutoff recurrence was under 10 Hz.

A channel gate shorted MOSFET called the MOS-bipolar gadget has likewise been proposed for use in enormous opposition execution [59]. For example, a PMOSFET works as a diode-associated PMOSFET with negative VGS; with positive VGS, the parasitic B1T is enacted and carries out a similar role. This method was utilized by Brr. Harrison et al. [601 to make a circuit with a low end recurrence. To diminish the bending of enormous result signals, two MOS-bipolar devices were connected in series, as delineated in Fig. 5. (c). The enhancer's end recurrence was 0.025 Hz, so, all in all the gadget's identical obstruction was more noteworthy than 1013 SL. The cerebrum recording enhancer given by Wattanapanitch et al. at [611] and the bioampli-fier proposed by Gosselin et al. at [621] both utilize this development. Moreover, Lim an at [531 introduced a high-pass channel with an end recurrence of 0.45 Hz using two oppositely coupled MOS-bipolar semiconductors and a 2-pF capacitor, which was said to have higher linearity than Harrison's game plan.

C. Circuits for Processing Various Physiological Signals are integrated into devices.

- Bioelectrical Signal Processing

Around the world, cardiovascular ailments are believed to be the primary executioners. It is doable to anticipate potential cardiovascular ailments through ECG checking. The ECG is a low recurrence, low sufficiency signal with a scope of 0.01-250 Hz and 0.5-4 mV [10]. Strong movement, sounds from the skin-terminal point of interaction, and different factors every now and again affect it. Intensifiers with high CMRR and low end frequencies are expected to view as the small differential sign. For ECG estimation, a few associations have delivered ICs. For little devices like pulse identifiers, Lasanen et al. [84] fabricated an ECG estimation chip in a 0.18-m CMOS process with a 1 V-1.8 V stock, 3 An arrived at the midpoint of current, and 82 dB CMRR. In this circuit, there were just two anodes, and the simple ground was created inside by the predisposition circuit. In a 0.35-m CMOS process, Wong et al. [85] executed an ECG estimating gadget utilizing a determined right-leg circuit. Albeit the determined right-leg circuit was initially based on a chip, the method of utilizing a cathode connected to the right leg as a source of perspective has been habitually utilized in discrete part circuits. Besides, Fay et al. [86] proposed an ECG processing speaker in a 0.5 um process with 2.8 W power utilization and 90 dB CMRR, which used a functioning establishing cathode to lessen 60 Hz commotion, feeble reversal

semiconductors to increment clamor proficiency, and capacitor-based intensification to improve coordinating. This design can accomplish the P, Q, R, S, and T wave attributes of an ECG.

- Acoustic Signal Processing

Severe metabolic, organic, and central nervous system diseases, as well as mortality, might result from the disruption of the regular breathing mechanism [93]. To track respiration and alert users when breathing stops, small wearable devices with low power consumption are required. A wearable breathing detector with a nanopower OTA-C band-pass filter has been proposed by Corbishley et al. [29] to capture the acoustic signal brought on by breathing. Only 70 nW were used by the filter, which was constructed using a 0.35-m CMOS technology and transconductance amplifiers driven at the subthreshold. Before being sent to the rectifier, low-pass filter, and comparator, the band-pass filter can first process the acoustic signal that the microphone has picked up. The system determines whether respiration is detected by comparing the processed signal with a predetermined threshold. If the device becomes loose or if respiration stops, an alert signal can be transmitted.

- Physical Quantity Processing

Heart rate, cuffless blood pressure, and SpO measurements were all performed using photoplethysmography, a non-invasive technique used to assess arterial volume changes. The photoplethysmogram (PPG), a very low frequency signal (0.5 to 17 Hz), has a ratio of AC to DC components of only 0.001 to 0.015 [104, [105]. Ambient noise and motion artifacts can easily upset him. By processing PPG, Wong et al. [75] introduced a near-infrared heart rate monitor chip. This circuit uses a low-pass current steering filter similar to the one described in Section III to achieve a cutoff frequency as low as 0.25 Hz without off-chip components. This is the first PPG processing chip.

Chemical Quantity Processing Compound sensors in light of particle delicate field impact semiconductors (ISFETs) have been usually used to evaluate particle fixation. An ISFET is a MOS semiconductor that has the gate association disengaged from the gadget as a kind of perspective cathode put into an answer of water that comes into contact with the gate oxide [107]. Both in the solid reversal zone and the feeble reversal locale, the channel current of the ISFET might be addressed as an element of hydrogen particle focus [108]. A silicon pancreatic beta cell, for example, was proposed by Pantelis et al. [109] and utilized for continuous glucose checking and insulin discharge in the treatment of diabetes. The silicon beta cell has a deliberate power utilization of 4.5 W and was made utilizing the UMC 0.25-m CMOS innovation. At this review, the metabolic exercises were displayed utilizing an ISFET one-sided in the subthreshold range. As per the response of glucose with the compound, a balanced connection between hydrogen particles and glucose particles can be constructed. The connection between the glucose particle focus and the channel current of the ISFET might be laid out using the connection between the hydrogen particle fixation and channel current of an ISFET.

2. LITERATURE REVIEW

The basic design of CFTA comes from the CDTA circuit, which is widely used in current mode analogue signal processing applications [5]. 5 Current Differencing Unit (CDU) and OTA stages are the two stages of the CDTA. By adjusting bias current IB, CDTA can offer electrical tuning of its transconductance. Due to its adaptable and flexible properties, CDTA is one of the best ABBs for creating current mode analogue signal processing applications. In the literature, there are numerous CDTA-based applications, including filters [40–42], oscillators [43–45], rectifiers [46], and multiplier/square rooter circuits [47]. However, many CDTA-designed applications do not make use of both input ports (n or p), which could cause noise to enter a monolithic circuit. By replacing the CDU of the CDTA block with the Current Follower (CF) stage, these problems can be resolved. As a result, a new ABB called CFTA is created [48, 49]. There are two stages: CF and TA. Herencsár et al. introduced CFTA for the first time in 2009, and the transistor model parameters NR100N (NPN) and PR100N were used to create the circuit (PNP). CFTA was created using the AD844 (as CF) and MAX435 (as TA) commercially available integrated circuits, as shown in [50]. A CMOS-based Multiple Output CFTA (MO-CFTA) operating at a supply voltage of 2.5V was introduced in 2009 [51]. One current input (p), three current outputs (x), and an accessory terminal (Z) make up MO-CFTA. In [52], Current Controlled CFTA (CCCFTA) was introduced. It uses a second generation Current-Controlled

Conveyor (CCCII), a grounded Y-terminal, and a balanced output OTA and operates at a supply voltage of 1.85 V. It is possible to electronically regulate the input parasitic resistance Rf of the CCCFTA. CFTA was demonstrated in [53] utilising bipolar transistors and a supply voltage of about 3V. Bipolar transistor- and CMOS-based CCCFTA circuits that functioned at a 2V supply voltage were introduced in [54] and [55], respectively. It was demonstrated in [56] how Z copy CFTA (ZCCFTA) was accomplished utilising CMOS technology. It operates at a supply voltage of about 1.5V and relies on an OTA with numerous outputs and a PMOS differential pair functioning as the CF. The ZC terminal on the ZC-CFTA replicates the current on the Z port. Bipolar ZC-CFTA was introduced in [57] and runs at a supply voltage of about 3V. A new ZC-CFTA implementation in CMOS that also performs at a 3V supply voltage was presented in [58]. This construction has incredibly low input resistance, though. The Modified Current Controlled Current Follower Transconductance Amplifier (MCCCFTA), which runs at a supply voltage of 1V, was 6 introduced in [59]. Two TA stages and one CCCII with the y terminal grounded make up this structure. Moreover, electronic control of the input parasitic resistance R for MCCCFTA is possible. Bipolar technology was used to implement Current Gain CFTA (CG-CFTA), which operates at a supply voltage of about 3V [60]. It consists of stages for balanced output transconductance amplifiers, current followers, and current mirrors with varying gains. This arrangement has the advantage of allowing for electronic tuning of the current transfer characteristics (iz/if and ix/iz) using external bias currents. The CFTA design described in [61, 62] was run at a supply voltage of about 1.25V. It is founded on an NMOS differential pair serving as both the CF and the OTA. The MO-CFTA, which uses bipolar technology and runs at a supply voltage of 1.5V, was introduced in [63]. This construction is built on two bipolar junction transistor-designed OTA and an NPN differential pair serving as a CF (BJT). A 1.25V supply voltage CCCFTA circuit was introduced in [64]. A ZC-CFTA operating at a 1V supply voltage was presented in [65] and was made utilising CMOS technology. It was reported in [66] that ZC-CFTA developed using BiCMOS technology operates at a supply voltage of 1V. CFTA that can be digitally programmed was introduced in [67]. It comprises of a transconductor that is digitally controlled. The improved floating current sources (IFCS) structure-based CMOS implementation of ZC-CFTA was introduced in [68]. With a supply voltage of 0.9V, this construction can function. A CMOS-based CFTA that operates at a supply voltage of about 0.75V was presented in [69]. Numerous applications developed with CFTA are also documented in the literature, including filters [70–97], oscillators [98–104], simulators [105–107], multipliers [108, 109], square rooting circuits [110], rectifiers [111], and generator circuits [112-113].

Two high impedance input ports (p and n), one high impedance intermediate port (Z), and one low impedance output port (W-) are all present in the VDIBA circuit. It was presented by Herencsar et al. in 2011 [10] for applications involving analogue signal processing. It is becoming very popular because to its straightforward architecture and design. Transconductance Amplifier (TA), which transforms input voltage to output current that flows out at port Z, and Inverted Buffered Amplifier are the two stages that make up the VDIBA architecture (IBA). First, employing the commercially available, 5V-operating IC OPA860 was suggested for its implementation [11]. The voltage buffer and diamond transistor are both parts of the IC OPA860 [12]. VDIBA's CMOS implementation, which uses a supply voltage of 0.9V, was introduced in 2013 [13]. Its output stage is created by a unity-gain inverting buffer, and its input stage is produced by a dual input, single output OTA (Operational Transconductance Amplifier). Gupta et al. presented the FGMOS (Floating Gate MOS) based VDIBA architecture in 2015; it operates at a supply voltage of about 0.75V [14]. The FGMOS transistor is used in its implementation, and the resistive compensation approach is used to increase the bandwidth. The bulk-driven quasi-floating gate (BDQFG)-based VDIBA was released in 2016 and operates at a supply voltage of about 0.4V [15]. Its architecture was created utilising the level shifter current mirror and BD-QFG approach. The transconductance of this VDIBA, however, is only about 226 S. On the same chip, analogue and digital circuitry work together to create noise and interference. Fully balanced differential design of analogue circuits can solve these issues. Utilizing commercially available IC, FBVDBA was implemented [16]. It was stated in [17] that FB-VDBA implemented utilising BiCMOS technology operates at a supply voltage of about 0.75 volts. In 2013, Sotner et al. [18] revealed a CMOS version of

the fully balanced VDBA/VDIBA design that runs on a 1.2V supply voltage. The OTA and IBA stages of FBVDIBA have differential input and output. The literature also contains a number of applications created utilising VDBA/VDIBA/FD-VDIBA, including filters [19–23], inductance simulation circuits [24–29], capacitance multipliers [30–32], oscillators [33–38], and phase shifters [39].

3. RESULT & DISCUSSION

We used the AMI ABN 1.5-pm two-metal two-poly CMOS process to construct the amplifier. Designing the amplifier with C1 at 20 pF and 02 at 200 fF results in a gain of 100. For optimum linearity, CI and C2 were both constructed as poly—poly capacitors. The 17 pF nMOS capacitor used in the bandwidth-limiting load capacitor 01 was constructed. Capacitors occupy 67% of the 0.16 mm2 silicon space needed for one amplifier circuit. a die image of a 2.2 mm by 2.2 mm chip with six different amplifier designs.

Frequency	Gain (db)	Phase (deg)
10^{-3}	31	45
10^{-2}	33	44
10^{-1}	34	43
10^{0}	40	40
10^{1}	41	38
10^{2}	42	35
10^{3}	40	32

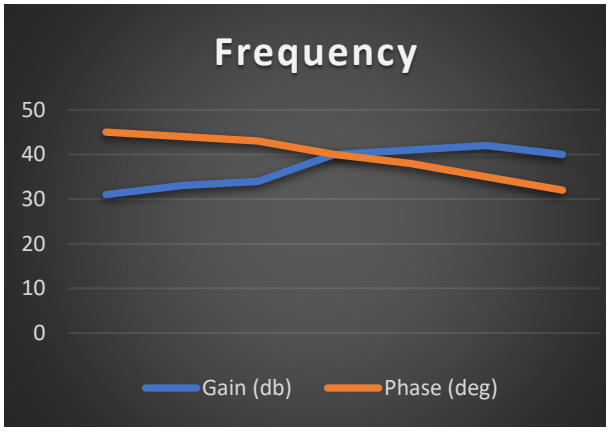

Figure.1: Measured transfer function of amplifier.

A. Testbench Results

the 0.004 Hz to 50 kHz estimated intensifier move capability. The midband gain is 39.5 dB, which is simply under our 40 dB design necessity. The little C2 capacitors' bordering fields, which bring about a higher capacitance than was pulled, are probably going to fault for this distinction. Around 0.025 Hz is where the low-recurrence cutoff ha is found. This is comparable to a gradual MOS-bipolar component opposition of r > 1013Q. The deliberate information alluded voltage commotion range is portrayed in Fig. 7. The lif commotion corner happens at 100 Hz, and the warm clamor level is 21 nVA. A runs commotion voltage of 2.2 iiVrms results from reconciliation under this bend from 0.5 Hz to 50 kHz. The result commotion waveform was recorded, then, at that point, separated by gain to make an information alluded clamor waveform with a runs worth of 2.2 iNrms. This commotion estimation was then confirmed. Startlingly, 1/f commotion isn't the circuit's principal wellspring of clamor. Input-alluded commotion in the circuit would be 2.1 Vrms if 1/f clamor were totally dispensed with. The use of pMOS input devices with enormous gate regions, as well as the relatively high warm clamor level of 21 nV/Hz are both contributing variables to the low commotion corner. Because of the circuit's restricted bandwidth and the need that input-alluded clamor just be not exactly the standard extracellular neuronal foundation commotion of 5-10 Vrms over this bandwidth, this commotion level is OK.

For inputs less than 16.7 mV top to-top, complete consonant mutilation (THD) stays below 1%. (bigger than run of the mill extracellular brain signals). Our dynamic reach is 69 dB on the off chance that we process it considering a mutilation cutoff of 1% (a moderate definition). Rather than utilizing two parts in series, we likewise made an alternate circuit utilizing only one MOS-bipolar pseudo resistor component .This speaker has a lower dynamic scope of 66 dB and 1% THD for a 12.0-mV top to-top information.

Both the power supply dismissal proportion (PSRR) and the well known mode dismissal proportion (CMRR) were estimated and viewed as higher than 80 dB. Crosstalk between speakers close to one another on the chip was estimated and viewed as 64 dB or less. Four enhancers' feedback alluded offset voltages, which went from 180 to 550 V, were estimated.

Comparing our amplifier's power-noise performance to estimated NEF values from previously published bio-amplifiers In comparison

to existing designs, the amplifier given here demonstrates a substantially improved NEF.

Table. Simulated and Experimental Characteristics of Neural Amplifier

Parameter	Simulation	Measured
Supply voltage	±3.5 V	±3.5 V
Supply current	16 μA	16 μA
Gain	40 dB	39.2 dB
Bandwidth	7.5 kHz	7.3 kHz
Low-frequency cutoff	0.130 Hz	0.028 Hz
Input-referred noise	2.1 $\mu Vrms$	2.2 $\mu Vrms$
Noise efficiency factor	3.9	4.0

B. Biological Test Results

To affirm that the circuit works when connected to a brain terminal, we utilized the bioamplifier referenced above as a preamplifier in a clear brain recording test. Utilizing a platinum-tipped extracellular microelectrode, we caught unconstrained neuronal action in the rodent olfactory cerebrum (Bionic Advancements, Salt Lake City, UT). We tracked down huge meddling signals at 60 Hz and around 50 kHz because of the unshielded wires associating the anode array to the speaker circuit. After the bioamplifier circuit, we constricted frequencies below 300 Hz and north of 30 kHz utilizing two single-pole channels. A recorded activity potential from this framework associated with the enhancer input is displayed. Top to-top sign and commotion levels delivered with our low-power framework are equivalent to those got with a rack-mount biosignal speaker framework that is promptly open (Bionic Innovations)

Devices	W/L (μm)	$I_p(\mu A)$	Inversion coefficient	$g_m/I_p(V^{-1})$	$V_{EFF} = V_{GS} - V_t(V)$
M_1, M_2	800.0/4.0	0.032	0.0034	27.1	-0.206
$M_3, M_4 M_5, M_6$	6.4/470.0	0.032	17	5.8	+0.304
M_7, M_8	6.4/104.0	0.032	11	7.0	+0.242
M_9, M_{10}	20.0/20.0	0.064	1.4	15.4	+0.059
M_{cascN}	12.0/3.2	0.032	0.063	25.7	-0.092
M_{cascP}	6.4/3.2	0.032	0.34	21.5	-0.017

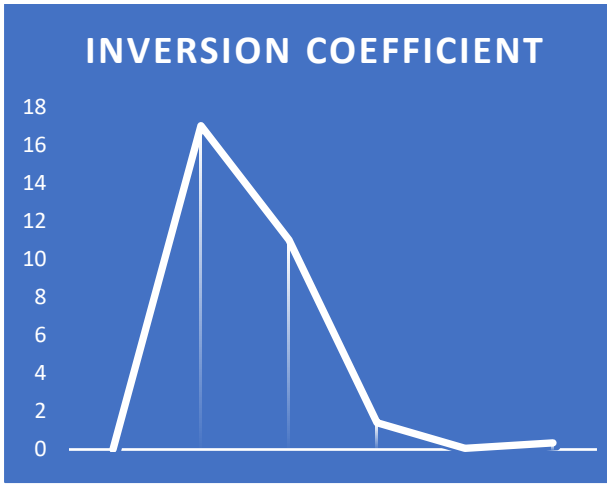

CONCLUSION

A 7.2-kHz bandwidth input-alluded commotion of 2.2 Vrms north of a 80 W completely integrated CMOS biosignal enhancer has been illustrated. The enhancer has no off-chip parts and rejects dc counterbalances regularly found in microelectrode recording applications while passing millihertz-range low-recurrence signals. We had the option to acquire the best power-commotion tradeoff among biosignal speakers by using the high level of devices working in subthreshold. Huge scope implantable cerebrum recording systems would be conceivable on the grounds that to a 1000-channel speaker that would require just 80 mW and fit on a 13-mm by 13-mm silicon kick the bucket in a 1.5-m process (cushions precluded). In an EEG speaker application, we utilized a similar design methodology and got a tantamount NEF at a fundamentally more modest bandwidth and power dissemination.

The baseband hardware of direct-change RF recipients could likewise utilize the low-recurrence ac coupling that the MOS-bipolar component gives. For low-power totally integrated collectors, the immediate change design is engaging, yet gadget

bungle and substrate coupling cause enormous dc balances that might be considerably greater than the gotten signal [29]. The speaker depicted in this article can be utilized in integrated direct-transformation systems since it accomplishes ultralow-recurrence ac reaction while altogether dismissing huge dc balances.

FUTURE SCOPE

The performance of nanoscale devices is superior to that of MOS devices. Devices using sub-micron technology operate with low supply voltage. Fast performance on chip neural recording devices will be made possible by features like high speed, high noise immunity, and less consumable space. Low power applications can make use of the FINFET, DGFET, MIGFET, and newer creations such the biochip, dust chip, and biosensor.

REFERENCES

1. P. Bonato, “Wearable sensors/systems and their impact on biomedical engineering,” IEEE Eng. Med. Biol. Mag., vol. 22, no. 3, pp. 18–20, May/Jun. 2003.
2. D. W. Ryoo, Y. S. Kim, and J. W. Lee, “Wearable systems for service based on physiological signals,” in Proc. 27th Conf. IEEE EMBS, Shanghai, China, 2005, pp. 2437–2440.
3. X. F. Teng and Y. T. Zhang, “M-health: Trends in wearable medical devices,” Chinese J. Med. Instrum., vol. 30, no. 5, pp. 330–340, Sep. 2006.
4. A. Lymberis, “Smart wearable systems for personalised health management: Current R&D and future challenges,” in Proc. 25th Ann. Int. Conf. IEEE EMBS, Cancun, Mexico, 2003, pp. 3716–3719.
5. G. Tröster, “The agenda of wearable healthcare,” in IMIA Yearbook of Medical Informatics 2005: Ubiquitous Health Care Systems. Stuttgart, Germany: Schattauer, 2004, pp. 125–138.
6. J. E. Mezzich, “Psychiatry for the person: Articulating medicine’s science and humanism,” World Psychiatry, vol. 6, no. 2, pp. 65–67, Jun. 2007.
7. X. F. Teng, Y. T. Zhang, C. C. Y. Poon, and P. Bonato, “Wearable medical systems for p-health,” IEEE Rev. Biomed. Eng., vol. 1, pp. 62–74, 2008.
8. C. C. Y. Poon and Y. T. Zhang, “Perspectives on high technologies for low-cost healthcare,” IEEE Eng. Med. Biol., vol. 27, no. 5, pp. 42–47, Oct. 2008.
9. Y. T. Zhang, C. C. Y. Poon, and E. Macpherson, “Editorial note on health informatics,” IEEE Trans. Inform. Technol. Biomed., vol. 13, no. 3, pp. 281–283, May 2009.
10. J. G. Webster, Medical Instrumentation Application and Design. New York: Wiley, 1998, pp. 10–11.
11. T. M. Seese, H. Harasaki, G. M. Saidel, and C. R. Davies, “Characterization of tissue morphology, angiogenesis, and temperature in the adaptive response of muscle tissue to chronic heating,” Lab. Invest., vol. 78, no. 12, pp. 1553–1562, 1998.
12. E. H. Liu, G. M. Saidel, and H. Harasaki, “Model analysis of tissue responses to transient and chronic heating,” Ann. Biomed. Eng., vol. 31, no. 8, pp. 1007–1014, Sep. 2003.
13. Radio electronics: Battery technology overview [Online]. Available: http://www.radio-electronics.com/info/data/battery-technology/tutorial-basics-overview.php
14. M. H. Miles, “Recent advances in lithium battery technology,” in Proc. Gallium Arsenide Integrated Circuit (GaAs IC) Symp., 23rd Annu. Technical Dig., Baltimore, MD, 2001, pp. 219–222.
15. Alternative energy news: Battery technology [Online]. Available: http://www.alternative-energy-news.info/technology/battery-power/